NASA/TM—2013-217841

Ballistics Analysis of Orion Crew Module Separation Bolt Cover

Samuel A. Howard, Kevin E. Konno, Kelly S. Carney, and J. Michael Pereira
Glenn Research Center, Cleveland, Ohio

February 2013

NASA STI Program . . . in Profile

Since its founding, NASA has been dedicated to the advancement of aeronautics and space science. The NASA Scientific and Technical Information (STI) program plays a key part in helping NASA maintain this important role.

The NASA STI Program operates under the auspices of the Agency Chief Information Officer. It collects, organizes, provides for archiving, and disseminates NASA's STI. The NASA STI program provides access to the NASA Aeronautics and Space Database and its public interface, the NASA Technical Reports Server, thus providing one of the largest collections of aeronautical and space science STI in the world. Results are published in both non-NASA channels and by NASA in the NASA STI Report Series, which includes the following report types:

- TECHNICAL PUBLICATION. Reports of completed research or a major significant phase of research that present the results of NASA programs and include extensive data or theoretical analysis. Includes compilations of significant scientific and technical data and information deemed to be of continuing reference value. NASA counterpart of peer-reviewed formal professional papers but has less stringent limitations on manuscript length and extent of graphic presentations.

- TECHNICAL MEMORANDUM. Scientific and technical findings that are preliminary or of specialized interest, e.g., quick release reports, working papers, and bibliographies that contain minimal annotation. Does not contain extensive analysis.

- CONTRACTOR REPORT. Scientific and technical findings by NASA-sponsored contractors and grantees.

- CONFERENCE PUBLICATION. Collected papers from scientific and technical conferences, symposia, seminars, or other meetings sponsored or cosponsored by NASA.

- SPECIAL PUBLICATION. Scientific, technical, or historical information from NASA programs, projects, and missions, often concerned with subjects having substantial public interest.

- TECHNICAL TRANSLATION. English-language translations of foreign scientific and technical material pertinent to NASA's mission.

Specialized services also include creating custom thesauri, building customized databases, organizing and publishing research results.

For more information about the NASA STI program, see the following:

- Access the NASA STI program home page at *http://www.sti.nasa.gov*

- E-mail your question to *help@sti.nasa.gov*

- Fax your question to the NASA STI Information Desk at 443–757–5803

- Phone the NASA STI Information Desk at 443–757–5802

- Write to:
  STI Information Desk
  NASA Center for AeroSpace Information
  7115 Standard Drive
  Hanover, MD 21076–1320

NASA/TM—2013-217841

Ballistics Analysis of Orion Crew Module Separation Bolt Cover

Samuel A. Howard, Kevin E. Konno, Kelly S. Carney, and J. Michael Pereira
Glenn Research Center, Cleveland, Ohio

National Aeronautics and
Space Administration

Glenn Research Center
Cleveland, Ohio 44135

February 2013

This report contains preliminary findings,
subject to revision as analysis proceeds.

Level of Review: This material has been technically reviewed by technical management.

Available from

NASA Center for Aerospace Information
7115 Standard Drive
Hanover, MD 21076–1320

National Technical Information Service
5301 Shawnee Road
Alexandria, VA 22312

Available electronically at http://www.sti.nasa.gov

Ballistics Analysis of Orion Crew Module Separation Bolt Cover

Samuel A. Howard, Kevin E. Konno, Kelly S. Carney, and J. Michael Pereira
National Aeronautics and Space Administration
Glenn Research Center
Cleveland, Ohio 44135

Abstract

NASA is currently developing a new crew module to replace capabilities of the retired Space Shuttles and to provide a crewed vehicle for exploring beyond low earth orbit. The crew module is a capsule-type design, which is designed to separate from the launch vehicle during launch ascent once the launch vehicle fuel is expended. The separation is achieved using pyrotechnic separation bolts, wherein a section of the bolt is propelled clear of the joint at high velocity by an explosive charge. The resulting projectile must be contained within the fairing structure by a containment plate. This paper describes an analytical effort completed to augment testing of various containment plate materials and thicknesses. The results help guide the design and have potential benefit for future similar applications.

Introduction

In the wake of the United State's retirement of the Space Shuttle orbiter, NASA is developing a crew module, named Orion, under contract with Lockheed Martin to enable future U.S. manned space capability. The Orion Crew Module would sit atop a rocket in a configuration reminiscent of the Apollo-era vehicles. The rocket that will be used for launching the crew module into orbit is as yet undetermined, but may be a future commercial launch vehicle. Regardless of the launch vehicle used, a staged separation of Orion from the rocket will occur at some point in the launch. The first stage of separation includes jettison of the fairings (labeled as spacecraft adapters in Fig. 1) that sit below the crew module. The fairings are structural elements that support a portion of the launch loads, but also act as transition pieces between the crew module and the rocket, as well as covers for the lower part of the crew module and the service module beneath it. The service module provides propulsion to the crew module after separation from the main rocket for the final stages of ascent. It also contains various life support systems for the crew module from before launch up to the point just before reentry when it is jettisoned from the crew module. A conceptual sketch of the crew module, service module, and spacecraft adaptor can be seen in Figure 1.

The fairing jettison is achieved through the use of pyrotechnic devices, including separation bolts. The bolts are severed by a pyrotechnic charge and released with high velocity radially outward relative to the vehicle. The portion of the separation bolts ejected outward must be contained to avoid potential impact with other parts of the vehicle. Containment of these projectiles is accomplished through the use of plates that cover the access holes to the bolts. The location of the containment covers can be seen in Figure 2. An experimental program was developed at NASA Glenn Research Center to aid in the design of these containment plates. Various materials and plate thickness were tested in NASA's Light Gas Gun Lab for containment capabilities sufficient for the separation bolts. In a parallel effort, an analytical model of the containment plates and projectile were developed to aid in the design and potentially for future optimization. The analytical effort is outlined herein. The analysis discussed was carried out using Livermore Software Technology Corporation's, LS DYNA, a general purpose Finite Element Analysis (FEA) software package designed primarily for transient, nonlinear dynamics.

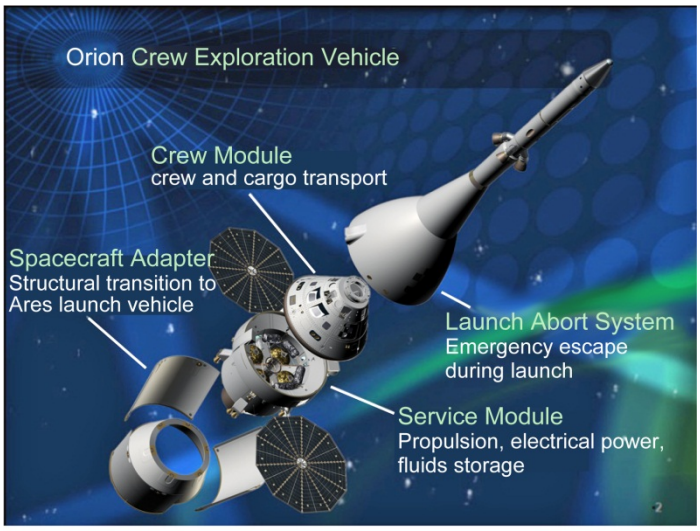

Figure 1.—Schematic of the Orion Crew Module and supporting systems. The fairings can be seen as the three semi-circular shells in the exploded view of the spacecraft adaptor. (Figure from NASA: JSC2009-E-145322)

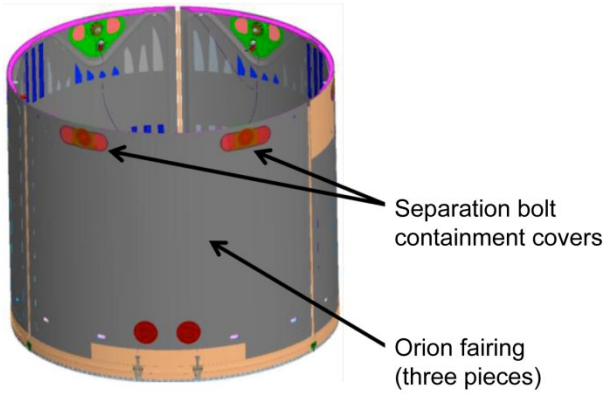

Figure 2.—Orion fairing schematic, showing the location of six separation bolt covers (two on each of the three fairings).

Containment Testing

As mentioned above, an experimental program was completed to test various containment plate thicknesses and materials. While the experimental program is not the focus of this paper, a brief description is included for comparison of results.

Three different materials were considered in the testing: Aluminum 6061 T6, Titanium 6Al-4V, and Stainless Steel 304. Several different thicknesses were tested as well. Stainless Steel was tested in 0.090, 0.119, and 0.224 in. (2.29, 3.02, and 5.69 mm) thicknesses; Titanium in 0.090, 0.127, and 0.277 in. (2.29, 3.23, and 7.04 mm) thicknesses; and Aluminum in 0.125 in. (3.18 mm). The objective was to determine a minimum thickness from available common sizes that would contain the projectile without failure (cracking without penetration was considered a failure).

A test fixture that mimics the flight hardware design (see Fig. 3) was placed in the Light Gas Gun Lab at the NASA Glenn Research Center (see Fig. 4). A separation bolt projectile (called a Superbolt) was fired at the target containment plate (from left to right in Fig. 3), while high-speed photography captured the event. For more on the operating procedures and capabilities of the test facility, see Periera (2003).

The mass of the projectile (5.78e-3 lbf s/in.^{2}/1001 g) in the tests matched the mass of the projectile expected in the flight conditions. The velocity of the projectile (169 ft/s/51.5 m/s) was set to 120 percent of the velocity expected under flight conditions to make the test somewhat conservative.

Results from the testing are reported in Table 1; tests 1, 9, and 10 are not included because the plates tested were a composite material and were beyond the scope of the analysis. Included are the target material and thickness, the profile of the projectile leading edge, the failure mode and comments. The profile of the leading edge refers to whether or not the projectile has so-called jacking screws or not. This is described in more detail in the analytical section.

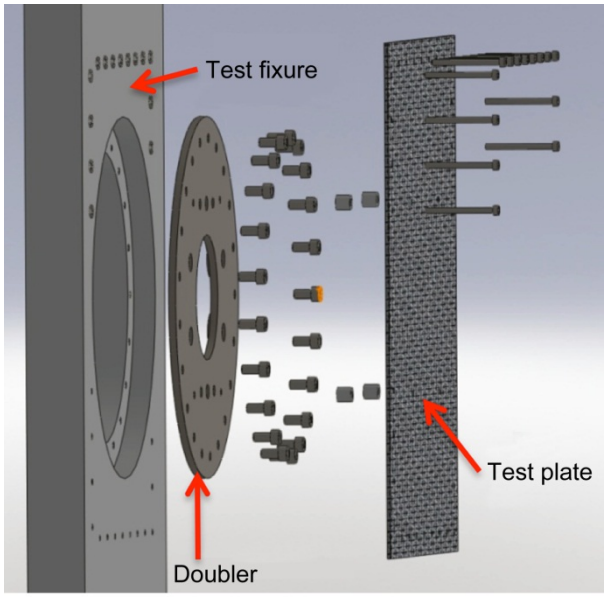

Figure 3.—Test fixture, doubler, and representative test plate; with exploded view.

Figure 4.—Light Gas Gun Lab, Building 49.

TABLE 1.—EXPERIMENTAL RESULTS

Test #	Ballistics lab test des. #	Target material, thickness	Projectile leading edge	Failure mode	Comments
2	LVG556	304 Stainless Steel (SS), 0.224 in. thick	1- 3/8 in. stud	No perforation	Plastic strain 0.444 in.
3	LVG557	304 SS 0.119 in.	1- 3/8 in. stud	No perforation	Plastic strain 1.009 in.
4	LVG558	Aluminum 6061 T6 0.125 in.	1- 3/8 in. stud	Aluminum perforated, stud penetrated through	no debris ejected, 1.113 in. plastic strain
5	LVG559	Titanium 6AL-4V 0.277 in.	1- 3/8 in. stud	Bolt shear at threads through nuts	Bolts, plate and projectile ejected: plastic strain: nil
6	LVG560	Titanium 6AL-4V 0.277 in.	1- 3/8 in. stud	No perforation	Plastic strain: nil
7	LVG561	Titanium 6AL-4V 0.127 in.	1- 3/8 in. stud	No perforation	Plastic strain: 0.28 in.
8	LVG562	Titanium 6AL-4V 0.090 in.	1- 3/8 in. stud	Plate perforated	No debris ejected Plastic strain: 0.3 in.
9	LVG563	304 SS 0.09 in.	3/8-24 bolts x8 grade 8	25 ft-lb	1- 3/8 in. stud
12	LVG566	Titanium 6AL-4V 0.09 in.	jackscrews	Plate perforated	No debris ejected. Strain: 0.426 in.

Containment Analysis

Assumptions/Modeling Procedures

Projectiles

Two different separation bolt projectiles were modeled in order to simulate the same conditions used for testing. The first separation bolt has no jackscrews, but has a 1 3/8 in. threaded rod protruding from the front. This projectile was used for the majority of the tests. The second separation bolt had six jackscrews protruding from the front. Figure 5 shows the first projectile and the corresponding model. Figure 6 shows the second projectile and its corresponding model. Both projectiles were modeled using a 10-node tetrahedron element formulation. The sabot (polycarbonate projectile carrier) was not included in the geometry of the projectile mesh, but its mass was included. In all cases, the side facing up in the figures is the impact side of the projectile.

Containment Plates/Armor Targets

The containment plates analyzed consisted of three different materials: 304 stainless steel, titanium 6Al-4V, and 6061-T6 aluminum. The thickness in each of the analyses matched the thickness in the corresponding test. The titanium doubler plate (Fig. 3) was included in the model because it was believed to be sufficiently flexible to be important in the overall stiffness of the system and therefore was important to include for the containment plate boundary conditions. Both plates were modeled with shell elements using the Belytschko-Tsay formulation with five integration points through the thickness. The outer diameter of the doubler plate was constrained in the translational degrees of freedom to fix the assembly in space. This constraint neglects the flexibility of the bolts attaching the doubler to the test fixture, and the flexibility of that structure, which is believed to be a reasonable assumption. In addition to the various materials and thickness tested, some of the tests used square plates with four bolts mounting the test article to the doubler. A second configuration used round plates with eight bolts. The number of bolts was increased due to bolt failures early in the test program (test #5). Figure 7 shows the test set-up for the square plates, and Figure 8 shows the corresponding FEA model. Figure 9 shows the test set-up and corresponding model for the round plates from the front. The back side looks the same as the square plates except for the addition of four more bolts.

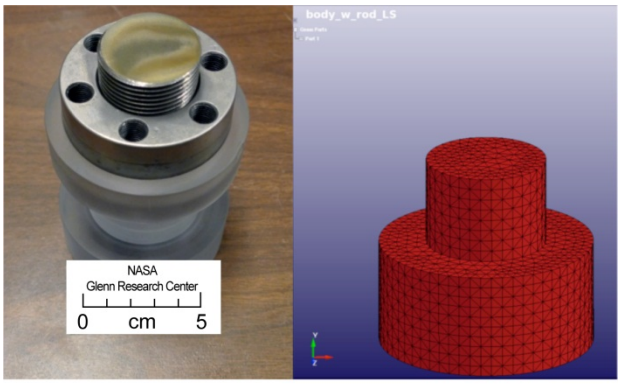

Figure 5.—Superbolt nut without jackscrews, shown with DYNA model.

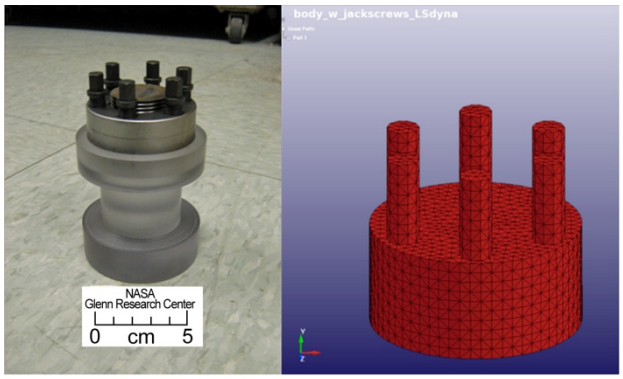

Figure 6.—Superbolt nut with jackscrews, shown with DYNA model.

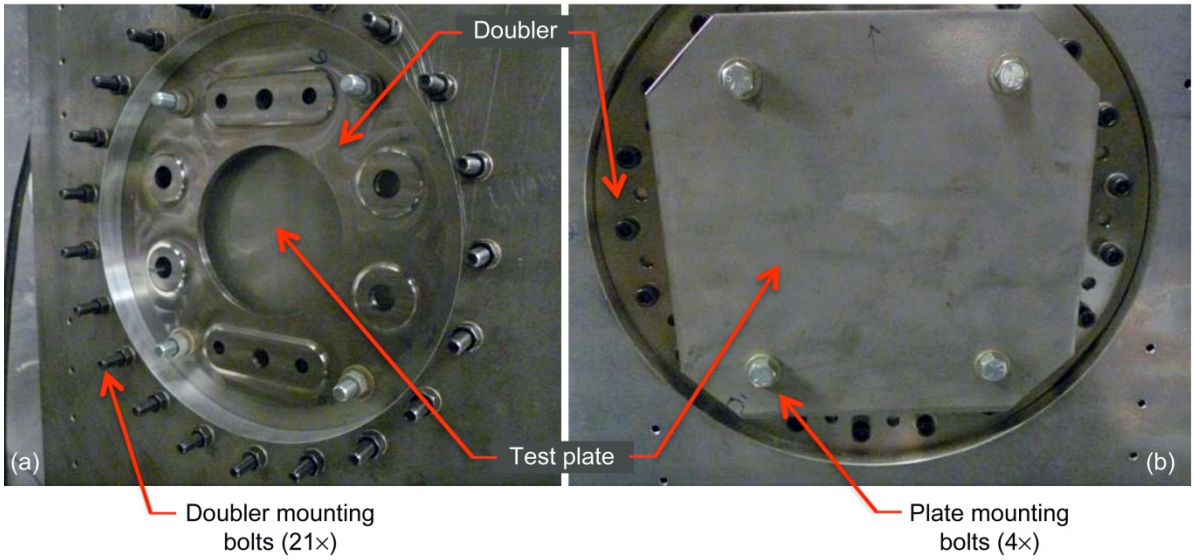

Figure 7.—Photographs of the test configuration with square plate. (a) Back side (impact side). (b) Front side.

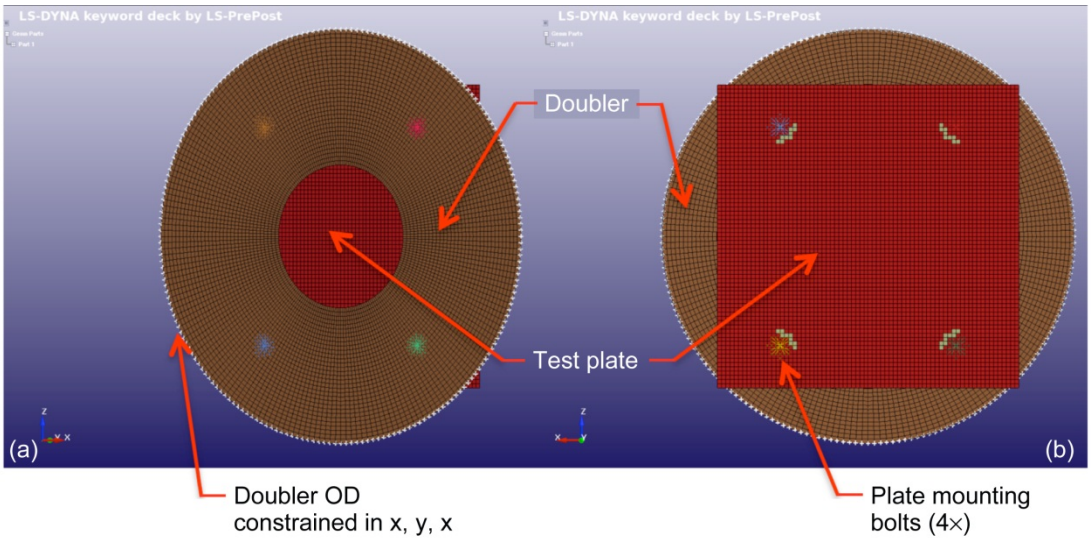

Figure 8.—FEA model of the test configuration with square plate. (a) Back side (impact side). (b) Front side.

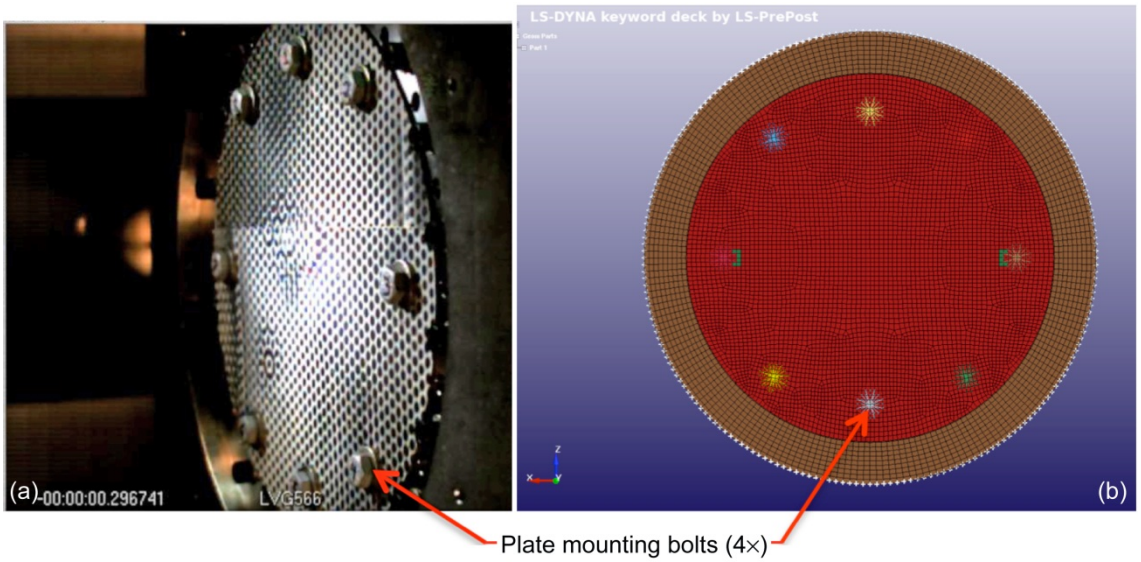

Figure 9.—Photograph and FEA model of the test set-up with the round plate. (a) Test set-up. (b) Model.

Mounting Bolts

The bolts mounting the containment plate to the doubler were modeled using beam elements. Each end of the beam was constrained to a set of nodes on each respective plate in a circular pattern representative of washers that were used in the tests under the bolt heads and nuts. The set of nodes were constrained as rigid bodies such that all six degrees of freedom of each node were locked with respect to one another. This resulted in a more rigid constraint than is thought to be present as it does not allow for any strain around the bolt holes. It also required relaxing the failure criteria of some of the elements adjacent to the rigid nodes due to unrealistically high plastic strain. The elements affected appear as a different color than the rest of the plate (for example, the green elements in the red plate on the right side of Fig. 8). Essentially, this constraint forces the plates to fail in the impact zone, if they fail at all. The local deformations in the areas immediately surrounding the bolts are probably low due to the stiff constraint, but the overall global deformations are comparable to the test results with reasonable agreement. Since none of the plates failed at the bolts during testing, this simplification is thought to be acceptable. The bolt model could possibly be improved in the future if needed.

Failure Criteria

The technique for predicting if the plates will contain the projectile is based on plastic strain to failure. If the plastic strain to failure is exceeded in a given element, the element will erode, or fail. In the case of dynamic FEA analysis, the plastic strain to failure depends on several parameters including mesh size, strain rate, state of stress, etc. Therefore, it is dependant not only on the material itself but also on the loading conditions to which the material is exposed. As a result, unless previous experiments have been performed where the material is similarly loaded and the material properties are measured, then the material model must be empirically calibrated with test results under similar loading conditions. In this test program not enough tests were done to fully characterize all the materials. The titanium target material was the only one in which both failure and non-failure was observed in testing. Therefore, it is the only material for which an attempt could be made to predict minimum thickness using LS DYNA, as discussed later.

Analysis Results

The analytical results augment the experimental results by quantifying several unknowns in the experiment. These quantities can provide a "sanity check" for hand calculations used for sizing bolts and preliminary pate thickness. In addition, the analysis could be extended in the future with additional testing if other materials or geometries are considered. The maximum axial force in the bolts, maximum impact force between the projectile and the plate, plastic deformation (plastic strain), time to maximum deformation, and total time for the impact event are all calculated in the model. The plastic deformation, time to maximum displacement, and impact time are estimated from test data as well, and compared to the analytical results. In addition, it is possible that future analysis can help optimize the containment by predicting the minimum required thickness to prevent failure of a given material with some additional testing to fully characterize the material model of interest.

Test numbers 1, 10, and 11 were not analyzed because they contained carbon fiber composite plates either alone, or in combination with metallic plates. Modeling the carbon fiber composite plates was not attempted due to a lack of an adequate material model. The remaining analytical results are listed below in Table 2.

The maximum impact force in column one is the peak force between the projectile and the plate, which in most cases occurs very early during the impact, see Figure 10 for a representative plot. For LVG561, LVG562, and LVG566, two peak force values are listed because the force peaked twice in those cases, see Figure 11. In test LVG561, the first peak occurred upon impact, the contact force decreased, followed by a second larger peak in force. In test LVG562, the first contact occurred upon impact, followed by a fracture of the plate, and corresponding decrease in contact force to zero. Then, as the larger diameter cross section of the projectile contacted the plate, a second impact occurred with a corresponding higher contact force.

In the cases with square plates and four mounting bolts, the axial force in the bolts tended to be similar in all the bolts. In the cases with the round plate specimens and eight bolts, the bolt pattern is not symmetric about the impact zone. That was simply due to other geometric constraints of the eight bolt pattern. Therefore, the bolts are not subjected to the same maximum axial forces. The convention in the table is to list the force followed by the number of bolts experiencing that force.

TABLE 2.—ANALYSIS RESULTS

Test #	Ballistics lab test des. #	Target material, thickness	Max. impact force (lb)	Max. axial force, bolts (lb)	Plastic deformation (analysis/test) (in.)	Time to max. displacement (analysis/test) (sec)	Impact time (analysis) (sec)
2	LVG556	304 Stainless Steel (SS), 0.224 in.	91,000	11,000	0.15/0.44	5.25E-4/7.81E-4	9.5E-4
3	LVG557	304 SS 0.119 in.	87,000	6,000	0.75/1.01	9.75E-4/1.24E-3	1.78E-3
4	LVG558	Aluminum 6061 T6 0.125 in.	32,500	3,500	1.00/1.11	7.00e-4/6.30e-4 (fracture)	7.00e-3 (fracture)
5	LVG559	304 Stainless Steel (SS), 0.224 in.	99,300	11,400	Nil/Nil	NA/N/A	7.90e-4
6	LVG560	Titanium 6AL-4V 0.277 in.	98,500	10,600(2) 8,000(2) 7,000(4)	0.10/Nil	3.70e-4/N/A	7.30e-4
7	LVG561	Titanium 6AL-4V 0.127 in.	33,000(1) 40,000(2)	6,000(2) 5,000(6)	0.30/0.28	5.45e-4/5.18e-4	1.05e-3
8	LVG562	Titanium 6AL-4V 0.090 in.	41,000(1) 38,000(2)	5,500(2) 4,200(6)	0.30/0.30	4.85e-4/4.82e-4 (fracture)	4.85e-4 (fracture)
9	LVG563	304 SS 0.09 in.	63,000	4,400(2) 3,700(6)	0.80/0.89	7.95e-4/5.18e-4	1.19e-3
12	LVG566	Titanium 6AL-4V 0.090 in.	30,000(1) 37,000(2)	6,000(2) 4,000(6)	0.25/0.43	4.85e-4/4.82e-4 (fracture)	4.85e-4 (fracture)

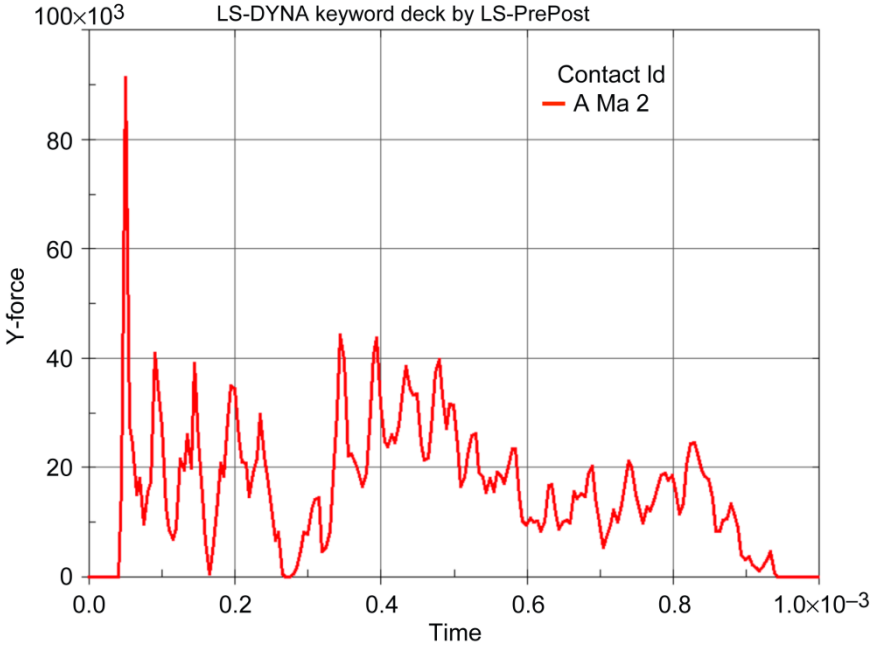

Figure 10.—Plot of contact force versus time for test LVG556. Contact force is representative of most impact cases.

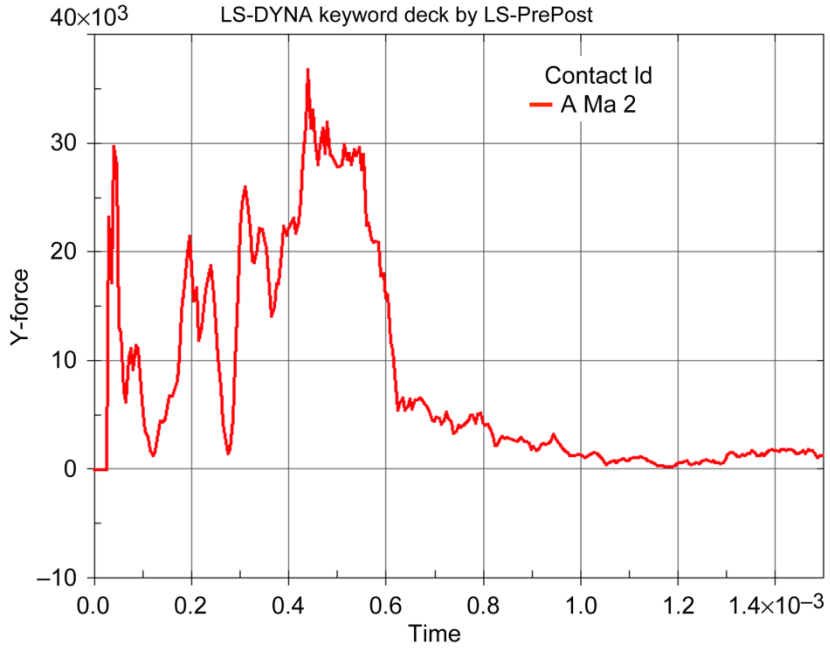

Figure 11.—Plot of contact force versus time for test LVG556. Contact force is representative of multiple impact cases.

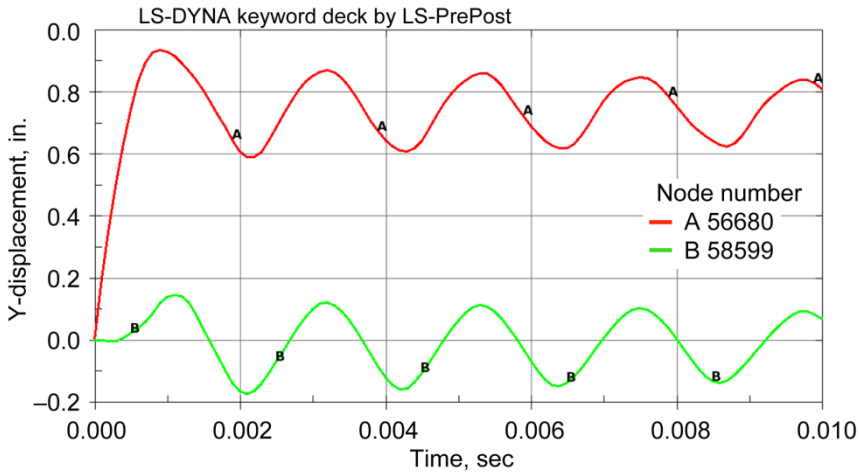

Figure 12.—0.119 in. SS304 (LVG557) plate displacement versus time of two nodes (A = node at the center of impact, B = node at the center of a bolt).

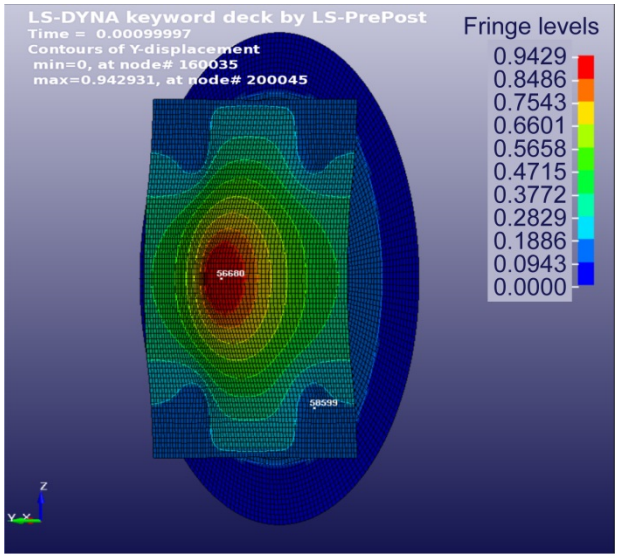

Figure 13.—Plot of 0.119 in. SS304 (LVG557) plate deformed shape and Y-displacement contours with two nodes identified (A = 56680 = node at the center of impact, B = 58599 = node at the center of lower right bolt) at maximum deflection, time = 0.001 sec after impact.

Plastic deformation in the analysis was taken as the distance from the center of the impact zone to the center of one of the bolt locations after the impact. However, the amount of time required for the vibration of the entire assembly to decay to zero was prohibitively long. To approximate the final deformation, the reasonable assumption was made that the plastic deformation occurred during the initial impact. Then, the DC offset of the vibration of the center point relative to the bolt location was taken as the plastic deformation. As an example, Figure 12 shows the displacement versus time for LVG557, the 0.119 in. (3.02 mm) thick SS304 plate with node 56680 at the center of the plate, and node 58599 near the center of the lower right hand bolt. Figure 13 shows the corresponding deformed shape and plastic strain contours at time t = 0.001 (near max displacement). Figure 14 is a frame from the video at approximately the time of maximum displacement for comparison. Figure 12 clearly shows a larger displacement for the first half

Figure 14.—Image of 0.119 in. SS304 (LVG557) plate at maximum deflection, time = 0.00124 sec after impact.

cycle at the center of the plate, followed by oscillation about approximately 0.75 in. (19 mm). The point at the center of the bolt oscillates roughly about zero because the bolt does not plastically deform during the event. So, for this case, 0.75 in. is taken as the permanent plastic deformation. The plastic deformations for the other cases are approximated similarly, except for the cases that fractured. For LVG558 and LVG562, in which the plate fractured, the deformation was taken as the DC offset between a node near the fracture location and one near the center of a bolt a long time after the impact. In all cases, this is thought to be a reasonable approximation for the plastic deformation.

Maximum displacement is not the same as maximum deformation because maximum displacement includes the plastic deformation of the plates and the maximum elastic deformation. Time to maximum displacement is a convenient parameter to compare between test and analysis because it is possible to estimate the time when maximum displacement occurs in the test videos even though the maximum displacement is not measured. It can then be compared to the predicted displacement of a node at the center of the impact in the analytical results.

Impact time is useful for quantifying the amount of time the two objects are in contact. It was only possible to obtain this quantity from the analysis, not the test results.

Overall, the analytical results and the test results compare well for plastic deformation and time to maximum displacement. The most notable difference is the plastic deformation of the 0.224 in. (5.68 mm) 304 stainless steel. For that case, the results are off by more than a factor of 2. Otherwise, the results are all within 20 to 30 percent. The actual deformations are always higher, which is consistent with the likelihood that the model is stiffer than the actual test hardware due to the rigid boundary condition on the doubler, the approximations in the bolt model, etc. The impact forces and bolt loads tend to be higher for thicker plates. Overall, the shape of the deformed plates in the analysis is consistent with the shape in the tests. Figures 15 to 21 are comparisons of deformed shapes for the various cases.

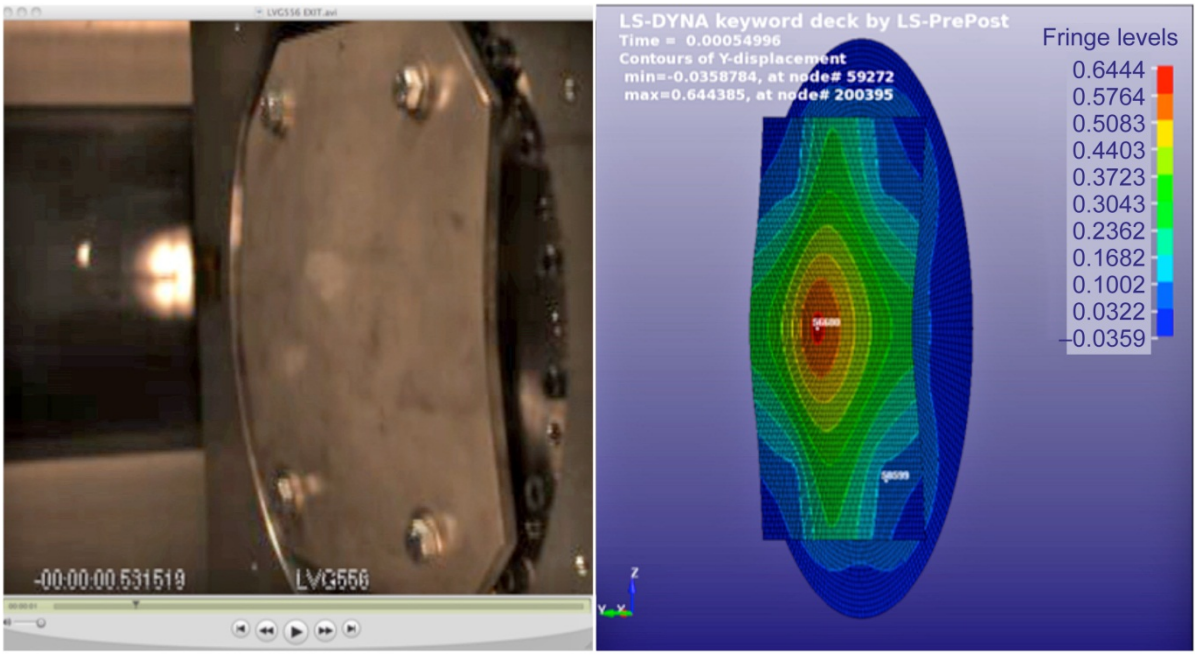

Figure 15.—LVG556 comparison of test video to analytical displacement at time of maximum displacement.

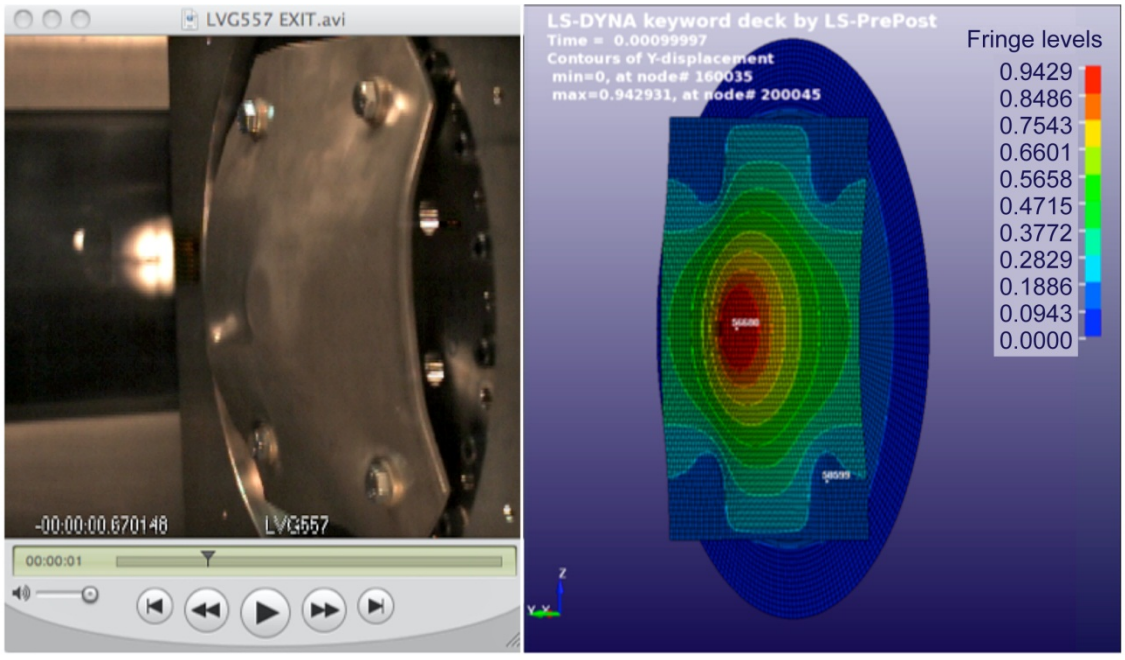

Figure 16.—LVG557 comparison of test video to analytical displacement at time of maximum displacement.

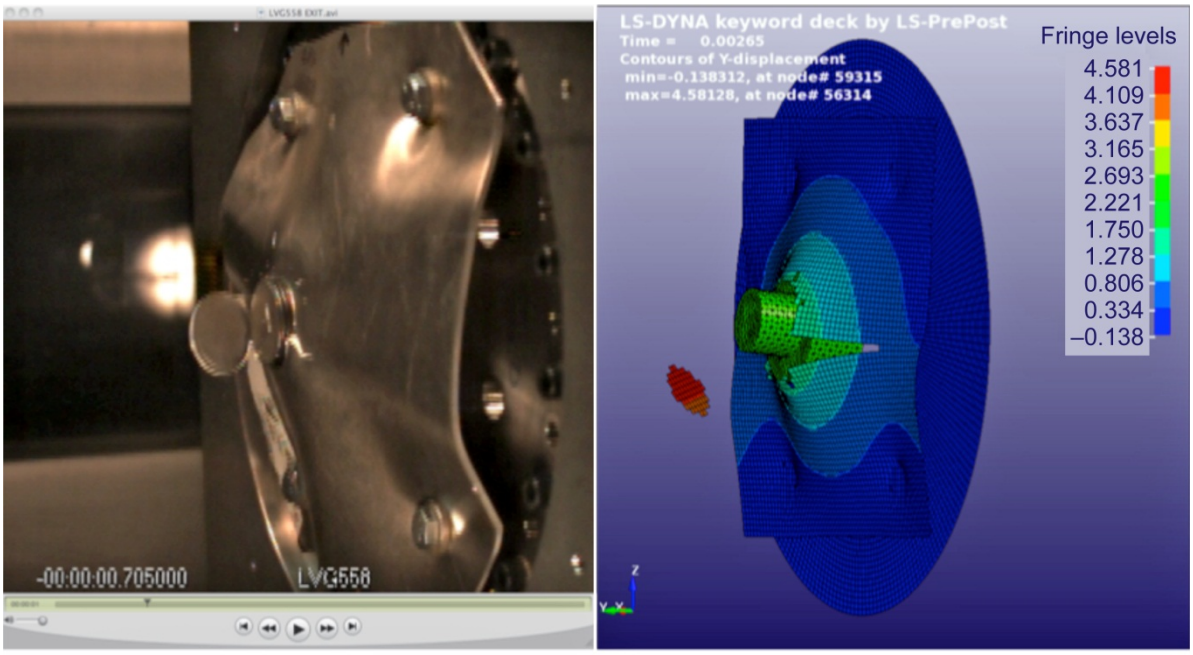

Figure 17.—LVG558 comparison of test video to analytical displacement at time of maximum displacement.

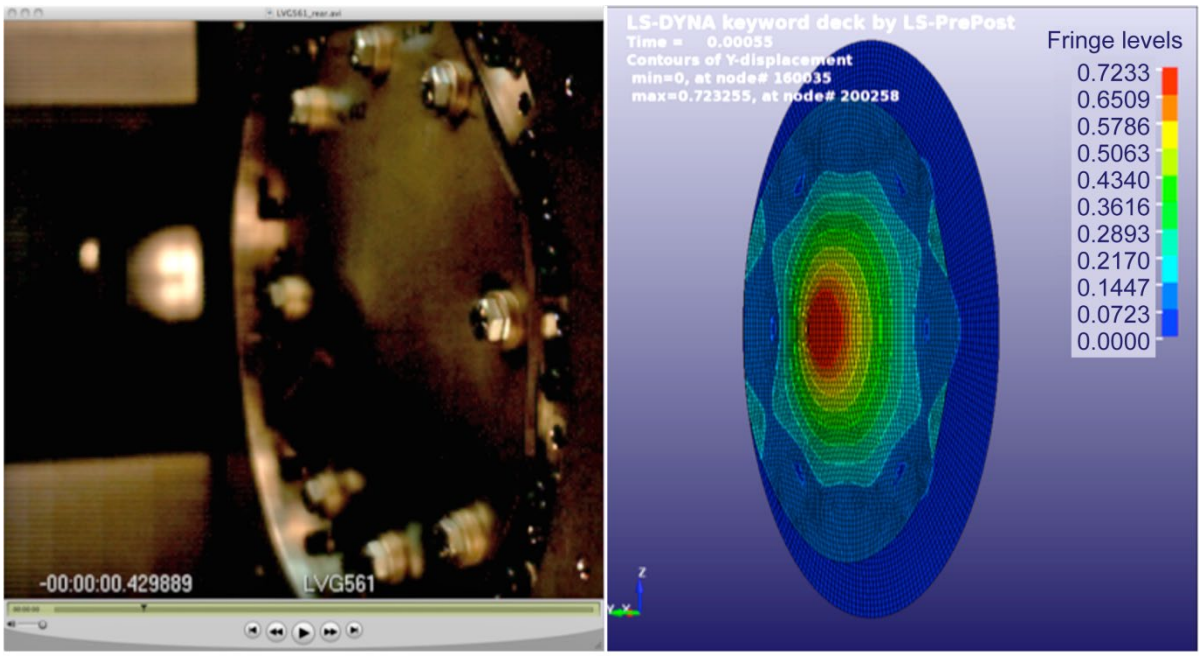

Figure 18.—LVG561 comparison of test video to analytical displacement at time of maximum displacement.

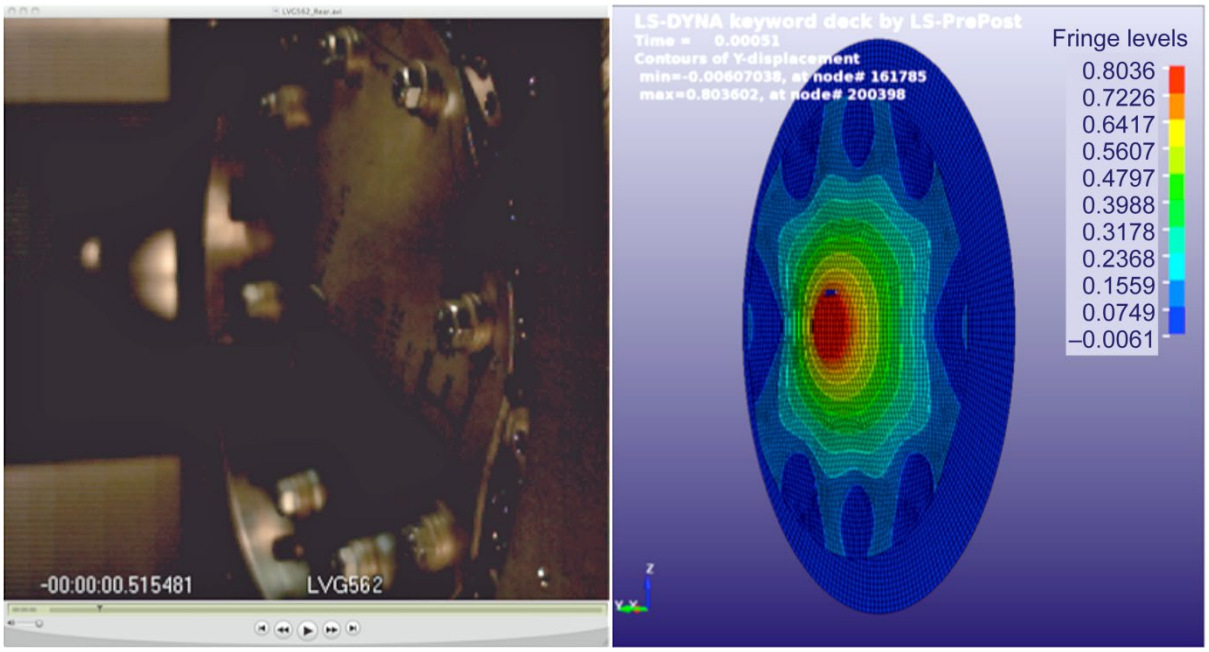

Figure 19.—LVG562 comparison of test video to analytical displacement at time of fracture initiation.

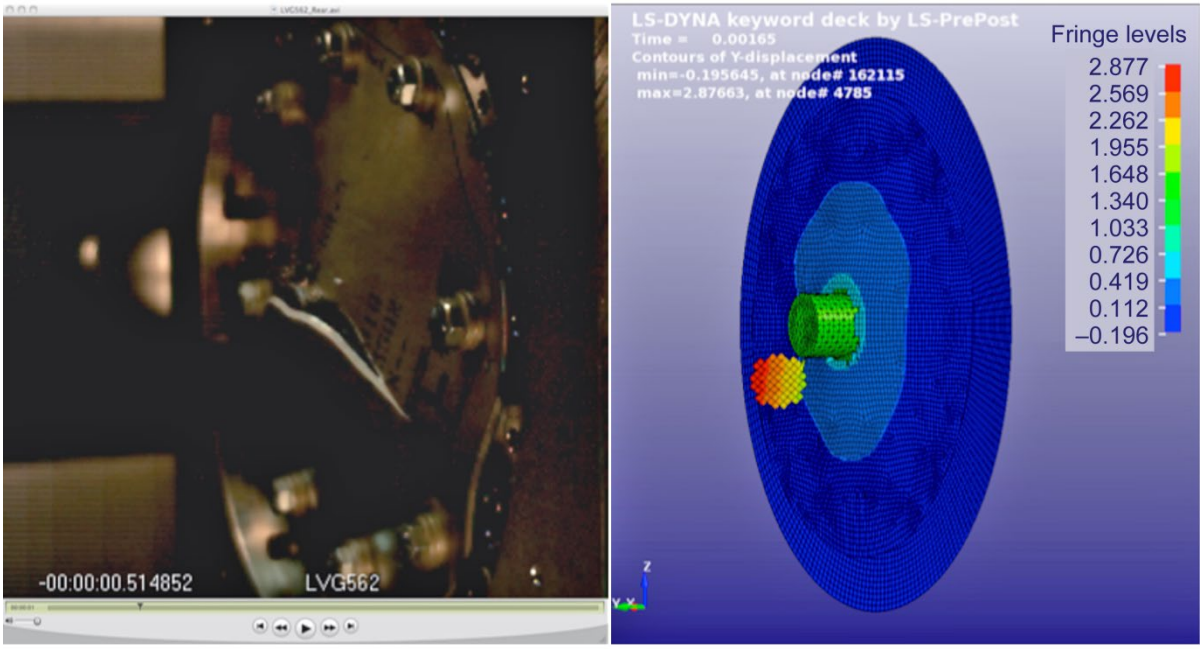

Figure 20.—LVG562 comparison of test video to analytical displacement at time of maximum displacement.

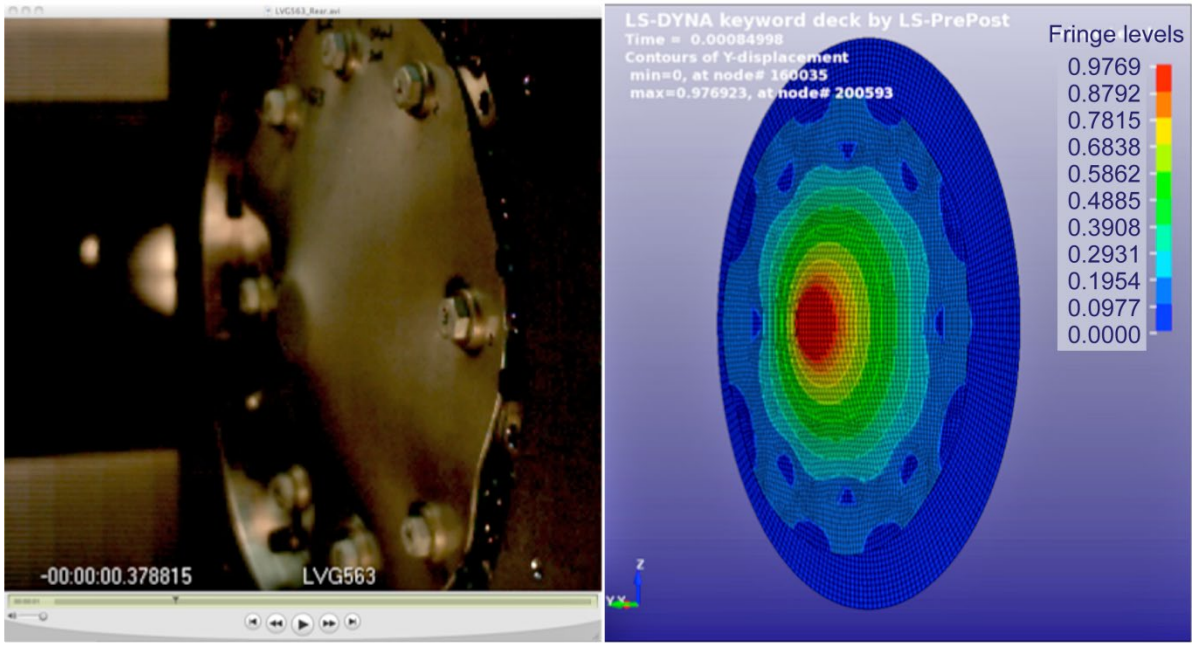

Figure 21.—LVG563 comparison of test video to analytical displacement at time of maximum displacement.

The titanium tests resulted in two plates that did not fracture from the impact, and one that did. This result can be used to determine the minimum thickness of titanium that could contain the projectile without fracture. The 0.127 in. (3.22 mm) thick titanium plate did not fracture, while the 0.090 in. (2.29 mm) titanium plate did. In order to bound the problem, the analysis was run with different plastic strain to failure values for both of these cases until the analytical model matched the test results. To observe failure in the 0.090 in. plate, a plastic strain to failure of 0.09 or less was required. To observe no failure in the 0.127 in. plate, a plastic strain to failure of 0.07 or greater was required. Therefore, if the plastic strain to failure is between 0.07 and 0.09, the analytical results match the test results, in terms of failure. To be conservative, the minimum value of 0.07 is used to determine the minimum thickness possible. It turns out that the thickness tested, 0.127 in. is likely to be very close to the minimum thickness that will not fail. According to the model, 0.125 in. (3.18 mm) will contain the projectile without fracture, 0.120 in. (3.05 mm) will contain the projectile, but will fracture. Therefore, 0.125 in. is likely to be a reasonable minimum thickness for titanium.

Conclusions and Recommendations

An analytic model of the containment plate arrangement specific to the geometry and constraints of the Orion Spacecraft Adaptor Fairing separation bolts was developed and shown to provide good agreement with the somewhat limited testing of candidate materials. Agreement between analysis and test was obtained by using a subset of the test results to quantify the material properties for the model. Sufficient testing and analysis was carried out to indicate that the model is capable of predicting the minimum thickness required for containment without fracture. Future optimization is possible with very little additional testing required for Stainless Steel and/or Aluminum.

In order to mitigate the release of any debris from the separation bolt firing and subsequently the Superbolt nut projectile released by this pyrotechnic event, a metallic containment plate of 0.125 in. Ti 6-4 or 0.09 in. 304SS has been shown capable to contain these projectiles safely in both a ground test or spaceflight environment, based on the testing and analysis performed to date.

References

Pereira, J.M. and Revilock, D.M., "The NASA Glenn Research Center Ballistic Impact Laboratory," 54th annual meeting of the Aeroballistics Range Association, Santa Fe, Oct. 2003.

REPORT DOCUMENTATION PAGE	Form Approved OMB No. 0704-0188

1. REPORT DATE *(DD-MM-YYYY)*	2. REPORT TYPE	3. DATES COVERED *(From - To)*
01-02-2013	Technical Memorandum	

4. TITLE AND SUBTITLE
Ballistics Analysis of Orion Crew Module Separation Bolt Cover

5a. CONTRACT NUMBER

5b. GRANT NUMBER

5c. PROGRAM ELEMENT NUMBER

6. AUTHOR(S)
Howard, Samuel, A.; Konno, Kevin, E.; Carney, Kelly, S.; Pereira, J., Michael

5d. PROJECT NUMBER

5e. TASK NUMBER

5f. WORK UNIT NUMBER
WBS 869021.05.03.03.15

7. PERFORMING ORGANIZATION NAME(S) AND ADDRESS(ES)
National Aeronautics and Space Administration
John H. Glenn Research Center at Lewis Field
Cleveland, Ohio 44135-3191

8. PERFORMING ORGANIZATION REPORT NUMBER
E-18615

9. SPONSORING/MONITORING AGENCY NAME(S) AND ADDRESS(ES)
National Aeronautics and Space Administration
Washington, DC 20546-0001

10. SPONSORING/MONITOR'S ACRONYM(S)
NASA

11. SPONSORING/MONITORING REPORT NUMBER
NASA/TM-2013-217841

12. DISTRIBUTION/AVAILABILITY STATEMENT
Unclassified-Unlimited
Subject Categories: 12, 18, and 39
Available electronically at http://www.sti.nasa.gov
This publication is available from the NASA Center for AeroSpace Information, 443-757-5802

13. SUPPLEMENTARY NOTES

14. ABSTRACT
NASA is currently developing a new crew module to replace capabilities of the retired Space Shuttles and to provide a crewed vehicle for exploring beyond low earth orbit. The crew module is a capsule-type design, which is designed to separate from the launch vehicle during launch ascent once the launch vehicle fuel is expended. The separation is achieved using pyrotechnic separation bolts, wherein a section of the bolt is propelled clear of the joint at high velocity by an explosive charge. The resulting projectile must be contained within the fairing structure by a containment plate. This paper describes an analytical effort completed to augment testing of various containment plate materials and thicknesses. The results help guide the design and have potential benefit for future similar applications.

15. SUBJECT TERMS
Containment; Ballistics; Separation

16. SECURITY CLASSIFICATION OF:			17. LIMITATION OF ABSTRACT	18. NUMBER OF PAGES	19a. NAME OF RESPONSIBLE PERSON
a. REPORT	b. ABSTRACT	c. THIS PAGE			STI Help Desk (email:help@sti.nasa.gov)
U	U	U	UU	22	19b. TELEPHONE NUMBER *(include area code)* 443-757-5802